Proceedings of the 21st ICSMGE, Vienna, Austria, 14 – 19 June 2026. Pistrol, Adam & Schweiger (eds.)
Published by: ÖGG, Austrian Society for Geomechanics, Salzburg, Austria, ISBN 978-3-9503898-4-5
https://doi.org/10.53243/ICSMGE2026-682

Cracking of the cover layer leading to backward erosion piping

Patricia Yida Tao, Huub de Bruijn, Benthe Charlie Noyons, André René Koelewijn, Ulrich Förster
Flood Defence Technology department, Deltares, Delft, the Netherlands, yida.tao@deltares.nl

Cor Zwanenburg
Soil Water Structures department, Deltares and Geo-Engineering Department, Delft University of Technology, the Netherlands

ABSTRACT: In the Netherlands, over 1300 km of the levees must be reinforced by 2050 as part of the Flood Protection Program. Innovative calculation techniques, driven by new knowledge, aim to optimize these reinforcement efforts. One of the dominant failure mechanisms that causes the required improvements is backward erosion piping. In assessing the probability of occurrence for this mechanism, the formation of an exit point in the cover layer is critical. The current assessment method does not explicitly account for the development of a crack in the cover layer. Including the cracking behaviour of the cover layer in the assessment framework would offer a more realistic and potentially more favourable evaluation of levee stability. Therefore, a comprehensive investigation was conducted, including a literature review, 13 geocentrifuge model tests, and two full-scale field tests. For the exit point formation of the cover layer, a physical description was written. This was primarily based on observed behaviour from the centrifuge tests. It was found that cracking started at the bottom of the cover layer, proceeding diagonally upwards to the toe of the levee. From there, an extended failure tree by backward erosion piping was drawn up. Next to cracking, other causes of exit point formation are possible, e.g. man-made holes or animal burrows. Field observations of sand boils were also incorporated into the analysis. This paper concludes with possible ways of an addition of the current assessment of uplift, differentiating between soil types, cohesion, tensile strength, and the thickness and volumetric weight of the cover layer.

KEYWORDS: Uplift, backward erosion piping, exit point, cover layer, cracking, levees.

1 INTRODUCTION: UPLIFT IN BACKWARD EROSION PIPING

In the Netherlands, over 1300 km (> 35%) of the levees must be reinforced by 2050 as part of the Flood Protection Program. Innovative calculation techniques, driven by new knowledge, aim to optimize these reinforcement efforts. One of the main failure mechanisms necessitating these required improvements is backward erosion piping, BEP.

In the safety assessment, the failure mechanism piping is considered to be split into three submechanisms, which need to occur sequentially: uplift, heave and backward erosion piping (CIRIA, 2013), Figure 1. First, uplift occurs when high water pressures in the aquifer act on the cover layer. This may cause cracking of the cover layer, leading to the formation of an exit point. Second, the heave process involves sand grains being transported vertically through the exit point by the upward flow of water. Third, with BEP, a form of internal erosion, a pipe will develop underneath the levee body and this may enlarge, potentially leading to instability of the levee body and inundation of the hinterland.

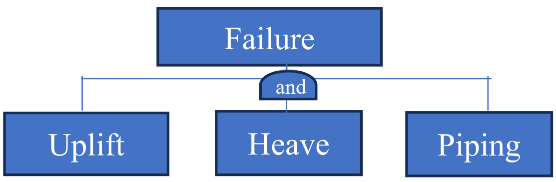

Figure 1. Three submechanisms of failure by backward erosion piping

In assessing the probability of occurrence of this failure mechanism, the formation of an exit point in the cover layer is a critical aspect. The current safety assessment method evaluates only the vertical force equilibrium at the exit point, considering the volumetric weight and the thickness of the cover layer, and the pore water pressures acting at its base. Under simplifying assumptions of one-dimensional conditions and neglecting shear stresses, this is a stress equilibrium. Alternatively, this equilibrium can be interpreted as situation in which the cover layer at the exit point has just detached from the underlying aquifer, resulting in zero effective stresses at its base, with the upward pore water pressure equalling the total downward pressure from the cover layer. In the Dutch guidelines (Rijkswaterstaat, 2021), the vertical equilibrium is assessed with the following formulas:

$$FoS = \frac{\Delta\Phi_{c,u}}{\Delta\Phi} \tag{1}$$

$$\Delta\Phi_{c,u} = \frac{d_{cover\ layer} * (\gamma_{sat} - \gamma_{water})}{\gamma_{water}} \tag{2}$$

$$\Delta\Phi = \Phi_{exit} - h_{exit} \tag{3}$$

In which:
FoS Factor of safety against uplift [-]
$\Delta\Phi_{c,u}$ Critical head difference over cover layer at exit point [m]
$\Delta\Phi$ Governing head difference over cover layer at exit point [m]
$d_{cover\ layer}$ Thickness cover layer [m]
γ_{sat} Saturated volumetric weight of cover layer [kN/m^3]
γ_{water} Volumetric weight of water [kN/m^3]
Φ_{exit} Head in aquifer at exit point [m]
h_{exit} Phreatic level or surface level at exit point [m]

The current safety assessment method does not explicitly account for crack development in the cover layer. Instead, it implicitly assumes that the exit point will form once vertical equilibrium has been reached between the upward pressure from the aquifer and the downward stresses from the self-weight of the cover layer. Incorporating the cracking behaviour of the cover layer in the assessment framework could yield a more realistic and potentially less conservative evaluation of levee stability. A more accurate assessment will lead to a more efficient design of reinforcement measures.

2 METHOD

A comprehensive investigation was conducted, which first resulted in an updated understanding of the failure mechanism, also known as physical description. This, in turn, led to a revised failure tree for backward erosion piping and a hypothesis on how to integrate the new insights into an optimized safety assessment.

The investigation consisted of multiple parts. There was a series of 13 geocentrifuge model tests conducted at the geocentrifuge facilities at Deltares, described by Zwanenburg et al. (2024) and Cengiz et al. (2024). For the cracking of the cover layer, the hypothesis was primarily based on observed behaviour from these centrifuge tests. Furthermore, two full scale field tests were performed at Reevediep, near Kampen, in the Netherlands. These geocentrifuge and field tests were supported by a literature review and extensive numerical simulations using finite element analysis. Field observations of sand boils, which indicate the occurrence of uplift, heave and possible backward erosion piping, thus exit point formation, were also incorporated into the analysis. In addition to cracking, other potential causes of exit point formation were also considered, e.g. man-made holes or animal burrows.

3 PHYSICAL DESCRIPTION OF EXIT POINT FORMATION UNDER UPLIFT CONDITIONS

The updated understanding of the failure mechanism was reported as a physical description of sequential phases. The physical description is summarised below.

3.1 *Load*

A high water level event determines the load on the levee system. For uplift, head levels in the aquifer will respond to the high water level and initially provide upward pressure to the cover layer. This will be the case until the pore water pressure at the top of the aquifer equals the total stress at the bottom of the cover layer. After this stage, the cover layer will deform slightly, and a gap between the aquifer and the cover layer will form. The pore water pressures in this water lens will determine the load.

3.2 *Uplift – floating phase and vertical equilibrium*

Generally, uplift is considered for the case that there is a vertical force equilibrium between the pore water pressure at the top of the aquifer and the self-weight of the cover layer, at the location of the exit point.

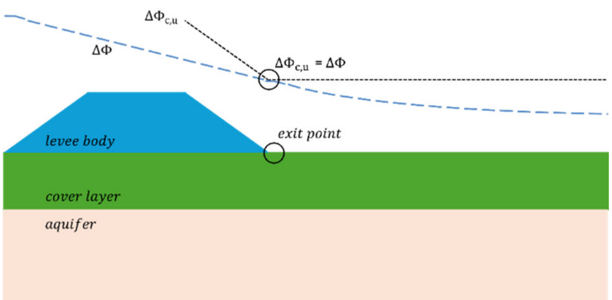

Figure 2. Conceptual drawing of uplift at vertical equilibrium

3.3 *Uplift – bulging phase and deformation cover layer*

When the water pressures rise after reaching the initial vertical equilibrium, an uplift zone will form. The cover layer will deform over the length of the uplift zone, leaving a small gap or 'water lens' between the cover layer and the aquifer. In this water lens, the hydraulic resistance is negligible, and the head at the top of the aquifer is horizontal. When the outer water level rises, this will lead to an increase in the length of the uplift zone. The head at the top of the aquifer will be slightly larger than the weight of the cover layer, because of the upward deformation of the cover layer.

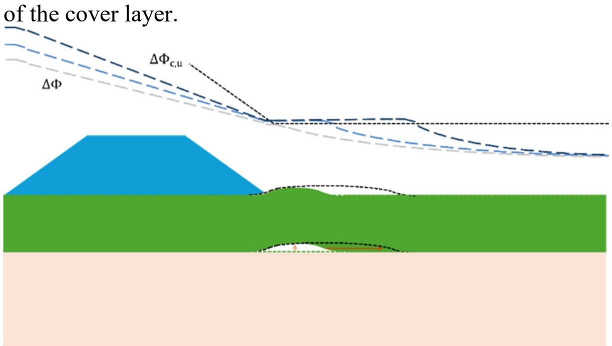

Figure 3. Conceptual drawing of deforming cover layer in uplift conditions.

3.4 *Uplift – cracking phase and forming of exit point*

The cover layer in the uplift zone will be subjected to stresses due to deformation. It was found that cracking started at the bottom of the cover layer, proceeding diagonally upwards to the toe of the levee. Spreading of the load of the levee explains why the crack does not start exactly vertically underneath the toe, resulting in a diagonal crack. Given the location of the crack and the observed cross-sectional behavior, these cracks are subjected to tensile stresses.

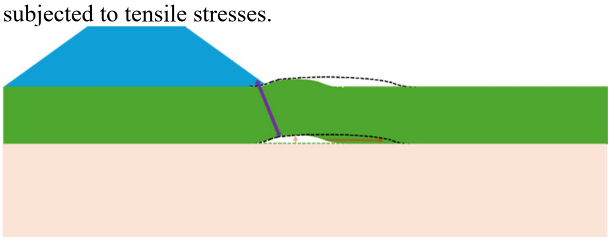

Figure 4. Conceptual drawing of cracking during uplift conditions

3.5 *Subsequent processes of backward erosion piping*

After the formation of the exit point, a well will occur. When the vertical gradient is high enough, the water will transport sand particles, also known as heave. Subsequently, backward erosion piping will occur, and a pipe (pattern) will be eroded. As soon as the pipe tip has connected with the external water, the erosion process will accelerate, and the pipe will enlarge. After this, the pipe will become unstable, leading the levee to lose its water retaining function.

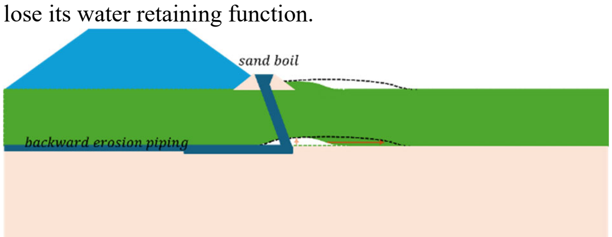

Figure 5. Conceptual drawing backward erosion piping

4 RESULTS

The results indicate that the cover layer provides additional resistance against crack formation under uplift conditions. The observations also confirmed the physical description and the associated conceptual phases. The results are split up in a few parts. Geocentrifuge tests revealed distinct, sequential phases in uplift behaviour. Key images and figures from the testing are included to support the physical description. This also includes the full-scale tests and further investigation of observed sand boils from a national dataset.

Table 1. Time of observations of start uplift and first report of diagonal crack in geocentrifuge models.

Test date (test number)	14-12-22 (5)	21-12-22 (6)	11-1-23 (7)	8-2-23 (8)	10-2-23 (9)	16-2-23 (10)	20-2-23 (11)
g-level	80	80	80	80	80	80	80
Cover layer thickness model scale (mm)	32	29	58	28	16	28	34
Cover layer thickness normal scale (m)	2.56	2.32	4.64	2.24	1.28	2.24	2.72
Start uplift (from photos) time after start data acquisition (HH:MM:SS)	04:03:27	05:14:50	12:17:29	05:47:12	01:18:58	00:16:04	00:10:50
Head standpipe levee-side at start uplift (cm)	18	18.4	22.1	23.1	18.2	24.5	21.4
Head standpipe hinterland at start uplift (cm)	17.4	17.4	20.9	14.7	14.1	15.7	14.9
First report of diagonal crack (from logbook) (HH:MM)	04:06	05:15	12:20	-	-	00:19	-
Start cracking (from photos) time after start data acquisition (HH:MM:SS)	04:05:53	05:15:49	12:20:20	06:44:36	01:25:01	00:18:37	00:12:21
Head standpipe levee-side at start cracking (cm)	19.3	19	23.8	23.8	20.6	25.5	22.3
Head standpipe hinterland at start cracking (cm)	17.9	17.2	20.6	14.8	14.1	15.7	14.9
Difference in head difference model scale (cm)	0.8	0.8	2.0	0.6	2.4	1.0	0.9
Increase in external water head difference normal scale (m)	0.64	0.64	1.60	0.48	1.92	0.80	0.72

4.1 *Geocentrifuge test series*

The geocentrifuge test series consisted of 13 tests with a uniform cover layer of remolded silty clay overlaying an aquifer. Details of the centrifuge tests are reported in Zwanenburg et al. (2024). A sketch of the geocentrifuge model is included in Figure 6.

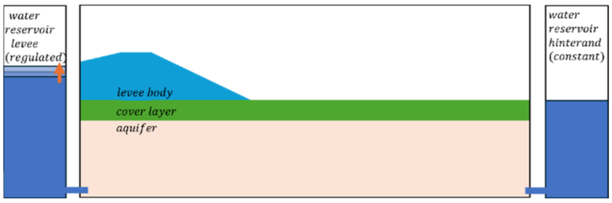

Figure 6. Sketch of the geocentrifuge model (side view).

4.1.1 *Observations during geocentrifuge testing*

In 11 of the 13 tests, a diagonal crack formed after an initial uplift phase, leading to heave and backward erosion piping, see also Figure 7.

The diagonal crack was present over the entire (in plane) length of the model. It is located at the toe of the levee, and the crack was observed to start at the bottom of the cover layer, propagating upwards. The diagonal crack consistently formed at an angle of approximately 60–65° from the horizontal direction. The length of the uplift zone was 15-45 m (187-559 mm on model scale). At the top of the cover layer, sand boils were observed at the location of the toe (Figure 8). Furthermore, in six of the tests, lateral cracks were observed, and in four of the tests, these sand boils occurred at the location of these lateral cracks.

4.1.2 *Analysis of onset of cracking*

For 9 of the 13 tests, the moment of uplift was determined. Two of these tests did not have a diagonal crack at the toe of the dike. For the remaining seven tests, the moment of crack-initiation was determined based on video data (Figure 9).

Table 1 shows there is a difference in time between the start of uplift and the start of cracking; there are few minutes in between. Using the photos of the test, the start of uplift and cracking was determined for seven of the tests. The external water head at the levee side and hinterland side was read from the standpipe. The difference in head difference was between

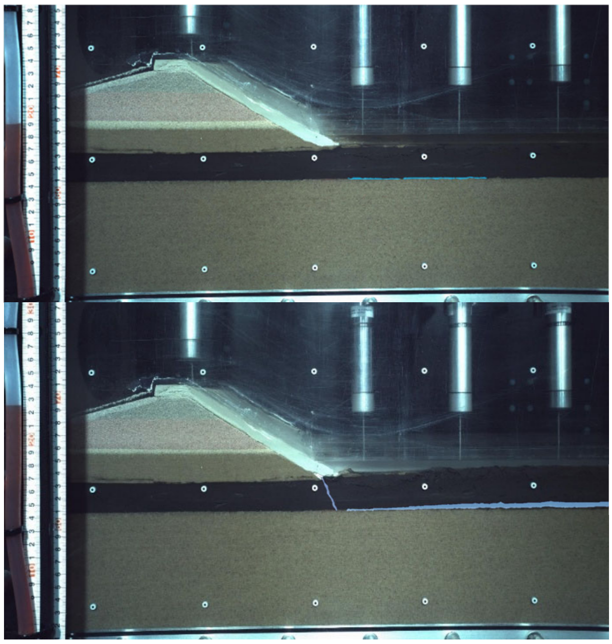

Figure 7. Geocentrifuge model (side view) with a clear distinction in the phases: in the top figure, only a water lens (colored blue) is visible without any cracks and in the bottom figure a higher external water level governs. There is a water lens and a crack at the toe.

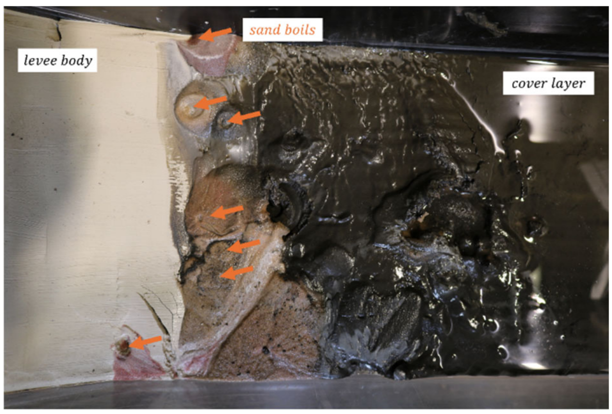

Figure 8. Geocentrifuge model (top view) with sand boils (indicated by orange arrows) located at the toe of the levee.

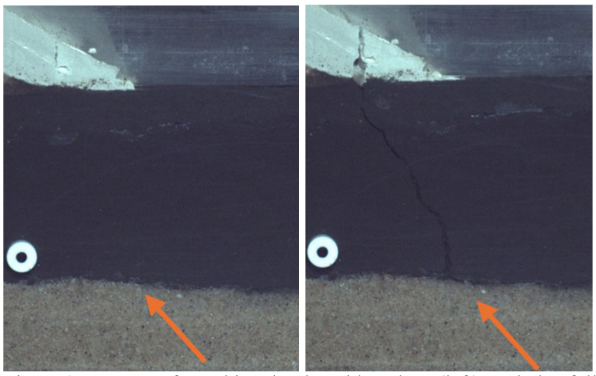

Figure 9. Onset of cracking in the video data (left) and the fully developed crack (right).

0.6-2.4 cm on model scale, which translates to 0. 5-1.9 m since the model was spun at 80g when the head was increased.

This difference is quite significant. The higher outer water level could be compared to the 'decimation height'. The definition of 'decimation height' is the average of the absolute difference between the design water level and the water level corresponding to a 10 times higher or lower probability of occurrence. For the Netherlands, the average decimation height equals to 0.46 m for the lower tidal estuary and 0.73 m for the upper river area (Witteveen en Bos, 2008).

The head difference against cover layer thickness is plotted in Figure 10. The hypothesis was that the thicker the cover layer is, the more resistance it would give to cracking. Unfortunately, there is no clear relationship found. It should be noted that for the test with a cover layer of 1.3 m, first a lateral crack was observed and from that crack a diagonal crack developed further. For the test with a cover layer of 4.6 m, it should be noted that the crack-initiation was observed but the crack did not fully propagate to the full thickness of the cover layer and did not lead to sand transport through the diagonal crack.

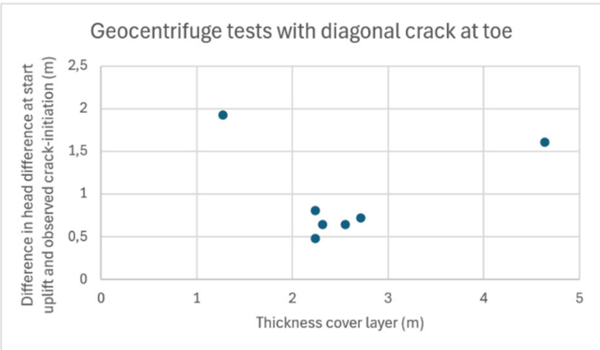

Figure 10. The head difference between uplift and cracking and the thickness of the cover layer during geocentrifuge tests with diagonal crack at toe (normal scale).

4.2 *Full-scale tests*

In the two full-scale tests, uplift conditions were reached over a period of several days, and the deformation of the cover layer was measured. The subsoil of the tests consisted of a cover layer of 3-3.5m of sandy clay and peat overlaying an aquifer. A comprehensive publication detailing the full setup, methodology and results of this field experiment, is currently in preparation.

Figure 11. Photo of full-scale test with pore water pressure meters at the front.

Sketches of the cross section of both tests and the deformations are shown in Figure 12 and 13. Test 1 consisted of a test area of 20 by 30 meters, which was surrounded by infiltration wells. The area prone to uplift in test 2 was 33 by 90 meters wide, and infiltration wells were at one side of the test area. In both tests, there were neither observations of cracking nor any sand boils. This supports the physical description, in the sense that cracking is a separate phase, and not, as it was assumed earlier, that it would implicitly occur simultaneously once uplift has been reached.

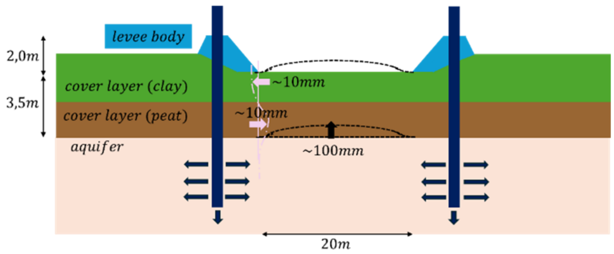

Figure 12. Sketch of full-scale test 1 conducted in July 2023.

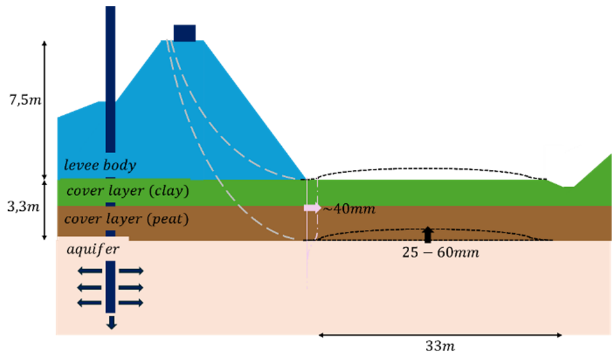

Figure 13. Sketch of full-scale test 2 conducted in August 2023.

It was found that the length of the uplift zone was 20-33 m, equal to the length of the excavation of the full-scale test location. The bottom of the cover layer had a vertical displacement of 25-100 mm.

4.3 *Sand boil database*

Field observations of sand boils connect to the physical description in the sense that both uplift and heave have occurred. Previous analysis of the Dutch national dataset (Figure 14), comprising over 800 recorded sand boils, showed a trend of fewer occurrences in areas with thicker cover layers (Figure 15).

Figure 14. Sand boil locations in the Dutch national dataset.

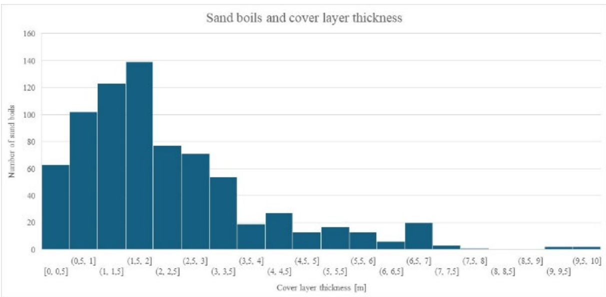

Figure 15. Sand boil observations sorted by cover layer thickness.

To further investigate the sand boils in thicker cover layers, a field investigation was conducted at selected locations where sand boils were recently reported (e.g. 2010) in areas without ditches and with a reported cover layer thickness greater than 4 meters. It was found that the available sand boil dataset and associated cover layer thickness data were of limited precision. Out of the five locations visited, the actual cover layer was significantly thinner than reported at three sites. At one location, it was concluded that uplift conditions likely had not been reached.

Sand boil observations from the national dataset cannot directly be used to distinguish between the different uplift stages: the 'floating' and 'cracking' of the cover layer. This is also simply because exit points may be formed due to different causes. In addition to crack formation under uplift (floating) conditions, other sources such as man-made holes or animal burrows are possible. A potential indication of poorly sealed soil investigations is when sand boil observations are evenly spaced, for example, every 100 meters along a linear infrastructure element, as can be seen along some underground pipelines.

Comparing sand boil observations with historical high water level data and design conditions is still valuable. By assessing whether uplift (floating) conditions occurred at the time of the observed sand boil, insight can be gained into its possible cause. If uplift conditions were never reached, it is impossible that crack formation under uplift conditions has taken place. However, if uplift conditions were reached, the historical high water level is close to the design water level and there have been no observations of sand boils, it means that cracking during design water levels is unlikely to happen. The last connection is that when uplift conditions were reached and sand boils observed, then the cracking phase has most likely occurred as well.

5 DISCUSSION

From the physical description, a translation to an addition on the failure tree by backward erosion piping is made. This addition provides the explicit consideration of exit point formation by cracking.

5.1 *Updated failure tree for sub mechanisms of backward erosion piping*

The uplift submechanism of piping could alternatively be considered as the formation of an exit point for (sand) boils and subsequently piping. The updated failure tree is shown in Figure 16.

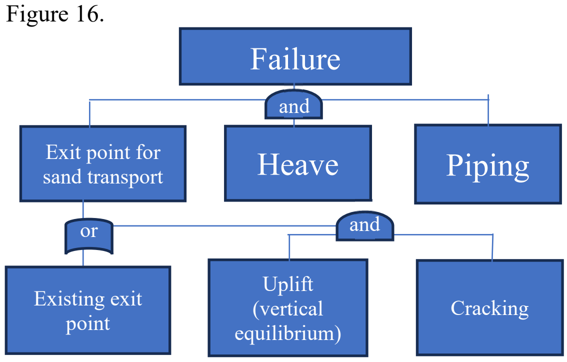

Figure 16. Extended submechanisms of failure by backward erosion piping.

5.1.1 *Existing exit point*

An assessment of uplift is not required if an exit point is deemed to be already present. This may be the case when no cover layer is present, or when the cover layer is quite thin. In this case, the cover layer is fully structured, especially if it lies above the mean ground water table, resulting in a high probability of existing holes. In addition, man-made holes or animal burrows could also be a cause of an existing exit point, if no mitigating measures are implemented. Lastly, observations of multiple sand boils in an area, also known as a 'field of wells', also justify the assumption of an existing exit point.

5.1.2 *Uplift vertical equilibrium*

The standard assessment of uplift consists of an assessment of the vertical equilibrium with design values. When using probabilistic methods, refinements could be implemented. This is, for example, a decrease in the average value of cover layer thickness and weight for thicker cover layers, as thick cover layers generally consist of multiple soil layers and the standard deviation will decrease due to averaging effects. A second example is to take the external water level statistics only up to the relevant range, that is to exclude water levels above the crest height as they do not lead to failure by backward erosion piping.

5.1.3 *Uplift cracking*

Assessing the resistance to cracking for the uplift submechanism would be an additional step. Using numerical simulations in finite element modelling is surrounded by uncertainties in load, (tensile) strength, propagation and localization of the cracks. However, the main assumptions concern the schematisation of the uplift zone, which are the length of the uplift zone, the pressure in the water lens.

A potential refinement to the uplift assessment would be to incorporate the conditional probability of cracking, given the uplift equilibrium has been reached. The strength of the cover layer comes from the thickness and soil type, and the corresponding volumetric weight, stiffness, and strength parameters.

5.2 *Potential refinements to uplift assessment*

5.2.1 *Using historical water level data*

Historical water level records could be used in two ways to assess uplift as a cause for exit point formation:

1. To exclude cracking as a possible cause of sand boil observations. This could be done by a back calculation of the historical uplift conditions at the time of the reported sand boils. If these calculations show that uplift conditions were never reached, cracking cannot have been the source, and the exit point must have formed through another mechanism.
2. To assess the likelihood of cracking, if uplift conditions have been reached before and there are no observations of sand boils. Here, the difference between the reached water level and the design water level plays a role, in combination with the height of the levee crest.

5.2.2 *Using geometry as possible addition to safety assessment*

The resistance to cracking is dependent on the thickness of the cover layer, since the stress capacity is higher against bending moments. Also, the resistance is dependent on the soil type in general and on strength parameters of the cover layer, such as the undrained shear strength, cohesion and tensile strength. In the geocentrifuge tests, remoulded silty clay was used. In reality, naturally deposited clays tend to have a higher resistance to cracking. It is expected that for peaty soils, the resistance to cracking is even larger due to the fibre structure in the peat.

5.2.3 *Possible assessment methods*

The likelihood of cracking could be assessed by expert judgement with an addition of the current assessment of uplift, differentiating between soil types, cohesion, tensile strength, and the thickness and volumetric weight of the cover layer. A table of verbal expressions linked to the change of occurrence is given below. These verbal expressions account for the chance of crack-formation given uplift (floating) conditions.

Table 2. Verbal expressions (ENW, 2012; Lacasse et al., 2007).

Verbal expression	Chance of occurrence (%)
Unlikely	<10%
Very unlikely	<1%
Almost impossible	<0,1%

Alternatively, one could make a qualitative assessment of all uncertainties in the assessment of the failure mechanism backward erosion piping, see Van der Linde et al. (2024).

6 CONCLUSIONS

New insights were gained into the sequence of events leading to the formation of an exit point due to uplift-induced cracking in backward erosion piping. Contrary to earlier assumptions within the safety assessment framework, reaching uplift (floating) conditions does not immediately lead to the formation of an exit point. Both geocentrifuge and field tests clearly support this conclusion. At the field tests, uplift (floating) conditions were reached over several days, without any visible sand boils, or cracks. In the geocentrifuge experiments, a distinct time delay and head difference was observed between the onset of uplift and the initiation of cracking. This difference typically was a few minutes, and the head level difference was between 0.6-2.4cm on model scale (equivalent to 0.5-1.9m at prototype scale under 80g conditions). These findings, next to a few geocentrifuge tests and field tests that did not crack at all, suggest that safety assessments should distinguish between uplift equilibrium and the likelihood of crack formation as separate phases within the failure process. Potential refinements include the use of historical water level data, sand boil observations, and expert judgement expressed in verbal probability terms to estimate the likelihood of crack-formation given uplift (floating) conditions or could make a qualitative assessment of all uncertainties related to the backward erosion piping failure mechanism. Ultimately, the final safety assessment should get a form which is supported by engineering practice.

7 ACKNOWLEDGEMENTS

The authors would like to acknowledge the financial support of National Flood Protection Programme (HWBP) and the water authority Drents Overijsselse Delta (WDOD). We also express gratitude to our Deltares colleagues, especially the centrifuge technicians, for making these experiments possible.

REFERENCES

CIRIA. (2013). The International Levee Handbook, Construction Industry Research and Information Association, CIRIA, publication C731, RP957. https://www.ciria.org/CIRIA/Resources/Free_publications/I_L_H/ILH_resources.aspx

Cengiz C., Cabrera M.A., Wittekoek B., Fransen M., Wopereis L., Zwanenburg C. (2024). Centrifuge tests on the uplift and deformation patterns of clay cover layers in deltas in: proc. XVIII ECSMGE 2024, Guerra N., Fernandes M.M., Ferreira C., Gomes Correia A., Pinto A., Sêco e Pinto P (eds) CRC Press/Balkema, Boca Raton, https://doi.org/10.1201/9781003431749-184

ENW. (2012). Technisch Rapport Grondmechanisch Schematiseren bij Dijken. Rijkwaterstaat Water, Verkeer en Leefomgeving.

Lacasse, S., Nadim, F., Uzielli, M. (2007). Hazard and Risk Assessment of Landslides. Proc. Geo-Denver 2007 Congress, Denver, Reston, ASCE.

Rijkswaterstaat (2021). Schematiseringshandleiding piping. WBI 2017. Versie 4.0. Ministerie van Infrastructuur en Waterstaat.

Van der Linde, L., Kanning, W., Van Beek, V. (2024) Beslissingsondersteunend raamwerk piping. Beschrijving en factsheets. 11209268-021-GEO-0001. Rijkswaterstaat Water, Verkeer en Leefomgeving.

Witteveen+Bos (2008). Decimeringshoogten TMR2006 RW1708-1 definitief. Deventer: RWS Waterdienst.

Zwanenburg C., Cengiz C., Fransen M.P., Wittekoek B., Wopereis L. (2024). Testing levee stability under uplift conditions; an experimental study in: proceedings of the 5th ECPMG 2024, (van Eekelen & Cabrera eds.) Delft